Published in final edited form as:
Nat Struct Mol Biol. 2016 August ; 23(8): 755–757. doi:10.1038/nsmb.3252.

FANCD2 limits replication stress and genome instability in cells lacking BRCA2

Johanna Michl[#1], **Jutta Zimmer**[#1], **Francesca M. Buffa**[1], **Ultan McDermott**[2], and **Madalena Tarsounas**[1,*]

[1]The CR-UK/MRC Oxford Institute for Radiation Oncology, Department of Oncology, University of Oxford, Oxford, U.K.

[2]Cancer Genome Project, Wellcome Trust Sanger Institute, Hinxton, UK

[#] These authors contributed equally to this work.

Abstract

The tumor suppressor BRCA2 plays a key role in genome integrity by promoting replication fork stability and homologous recombination (HR) DNA repair. Here we report that human cancer cells lacking BRCA2 rely on the Fanconi anemia protein FANCD2 to limit replication fork progression and genomic instability. Our results identify a novel role for FANCD2 in limiting constitutive replication stress in BRCA2-deficient cells, which impacts on cell survival and treatment responses.

Mutations in the breast cancer susceptibility gene 2 (*BRCA2*) predispose individuals to breast and ovarian cancer. As a result of compromised HR repair, *BRCA2*-mutated tumor cells differ from normal cells in their responses to exogenous DNA damage and to endogenous challenges that arise during DNA replication (e.g. at telomeres)1,2. This is due to the essential function of BRCA2 in protecting stalled replication forks against nucleolytic degradation3,4. A similar role in DNA replication has been ascribed to the Fanconi anemia group D2 protein (FANCD2)5 . FANCD2 is a central component of the Fanconi anemia pathway for DNA cross-link repair and its inactivation is associated with progressive bone marrow failure and cancer predisposition.

Recent work demonstrated that FANCD2 regulates responses to replication stress induced by mitomycin C (MMC) and hydroxyurea (HU)5–7. BRCA2 abrogation likewise triggers replications stress, a hallmark of BRCA2-deficient cancer cells that drives the associated pathologies8. This led us to investigate whether FANCD2 mediates replication stress

Correspondence should be addressed to M. T. (madalena.tarsounas@oncology.ox.ac.uk).

Author contributions

M.T., J.M., and J.Z. designed the study and the experiments. J.Z. and M.T. wrote the paper. J.M. and J.Z. performed the experiments. U.M. and F.M.B. analyzed *FANCD2* expression levels in cell lines and tumors, respectively.

Competing financial interests

The authors declare no competing financial interests.

Europe PMC Funders Author Manuscripts

responses in cells lacking BRCA2 and how this contributes to genome integrity and survival of these cells.

FANCD2 and BRCA2 are both required to prevent MRE11-dependent degradation of nascent DNA at stalled replication forks3,5. However, whether the two factors interact functionally with each other during this process has not been addressed. To investigate fork protection in cells lacking both FANCD2 and BRCA2, we transfected H1299 cells harboring doxycycline (Dox)-inducible shRNA against BRCA2 with siRNA against FANCD2 (Fig. 1a). We monitored replication fork degradation after prolonged HU treatment using DNA fiber analyses (Fig. 1b). Consistent with previously described roles of FANCD2 and BRCA2 in replication fork protection3,5, DNA tracks were significantly shorter in FANCD2- or BRCA2-depleted cells. Importantly, concomitant loss of FANCD2 and BRCA2 resulted in increased levels of fork degradation indicating that the two proteins mediated stalled fork protection by distinct mechanisms. Inhibition of MRE11 nuclease activity with mirin partially rescued degradation of nascent DNA in cells lacking FANCD2 and BRCA2, implicating MRE11 as one of the nucleases required for fork resection in this context.

Replication at stalled forks can be restarted by multiple mechanisms9. However, the roles of FANCD2 and BRCA2 in replication fork restart remain controversial3,5,10. In cells lacking FANCD2 or BRCA2, we observed impaired replication restart after HU treatment (Fig. 1c). This defect was more pronounced in cells deficient in both proteins, suggesting that FANCD2 and BRCA2 played independent roles in the restart of HU-arrested replication forks.

FANCD2 restricts DNA synthesis upon HU-induced replication stress in order to prevent accumulation of deleterious single-stranded DNA gaps7. BRCA2-deficient cells exhibit high levels of endogenous replication stress11, resembling that induced by HU treatment. To test whether FANCD2 limits DNA synthesis under replication stress conditions associated with BRCA2 inactivation, we measured replication rates in two BRCA2-deficient human cell lines treated with FANCD2 or control siRNAs. In both cell lines, FANCD2 depletion increased track length (Fig. 1d-f and Supplementary Fig. 1a), indicating that FANCD2 inhibits replication fork progression in the absence of BRCA2. Additionally, we observed an increase in origin firing in BRCA2-deficient cells lacking FANCD2 (Supplementary Fig. 1b) suggesting that FANCD2 suppresses activation of origins to prevent uncontrolled replication in the context of BRCA2 deficiency, similarly to HU12. Uncontrolled replication leads to DNA damage accumulation9. Consistent with this, in cells lacking FANCD2 and BRCA2 we observed enhanced levels of chromosomal aberrations (relative to single depletion, Fig. 1g,h), as well as elevated levels of γH2AX foci (Fig. 1i) that mark DNA damage sites. Thus, FANCD2 is required to prevent genomic instability in BRCA2-deficient cells.

DNA damage accumulation triggers DNA damage responses ultimately leading to senescence and apoptosis13. To determine whether the genomic instability observed in cells lacking FANCD2 and BRCA2 impacts on cell fate, we assessed apoptosis and senescence using Annexin V and β-galactosidase staining, respectively. We observed a significant increase in apoptotic, Annexin V-binding cells upon concomitant abrogation of FANCD2 and BRCA2 expression in H1299 cells relative to inhibition of each factor alone (Fig. 2a).

Likewise, FANCD2-, BRCA2-depleted primary MRC-5 human cells entered senescence at a higher rate than cells lacking either FANCD2 or BRCA2 (Supplementary Fig. 2) as measured using β-galactosidase staining.

Next, we investigated a potential synthetic lethality between FANCD2 and BRCA2. FANCD2 inhibition using two different siRNAs significantly decreased survival of H1299, DLD1 and MDA-MB-231 cells lacking BRCA2 expression in clonogenic assays (Fig. 2b-d and Supplementary Fig. 3a-d). Consistently, survival of DLD1 cells, in which FANCD2 expression was abrogated using the CRISPR–Cas9 technique, was significantly reduced by siRNA-mediated depletion of BRCA2 (Fig. 2e and Supplementary Fig. 3e). This indicated that FANCD2 is required for survival of BRCA2-deficient cells and suggests a synthetic lethal interaction between the two genes14. Depletion of the Fanconi anemia core complex component FANCA led to significantly impaired survival of BRCA2-deficient cells (Supplementary Fig. 3f) indicating that ubiquitination of FANCD2 is required in cells lacking BRCA2.

Interestingly, cell lines and tumors carrying *BRCA2* mutations exhibited higher *FANCD2* mRNA expression levels than cell lines and tumors with wild type *BRCA2* (Fig. 2f, Supplementary Fig. 4, Supplementary Tables 1,2). Thus far, no functional assays have been carried out to establish whether these mutations result in loss of BRCA2 function. However, our findings raise the possibility that *FANCD2* transcription is upregulated to sustain survival of BRCA2-deficient cells and tumors.

BRCA2 deficiency is commonly targeted by chemical inhibition of poly (ADP-ribose) polymerase 1 (PARP1) while Fanconi anemia patient cell lines are generally not sensitive to PARP inhibitors15. To address whether FANCD2 modulates the response to PARP inhibition, we treated H1299 cells lacking BRCA2, FANCD2 or both, with low doses of olaparib (Fig. 2g). Consistent with previous results15, this treatment was not toxic in the context of FANCD2 loss. However, we observed that FANCD2 abrogation enhanced sensitivity of BRCA2-deficient cells to olaparib, suggesting that FANCD2 mediates mechanisms of resistance to this drug.

In summary, we have demonstrated that FANCD2 is essential for cell survival in the absence of BRCA2. FANCD2 promotes DNA synthesis, replication fork protection and restart in BRCA2-deficient cells. This role of FANCD2 is analogous to that previously reported in response to exogenously induced replication stress (e.g. HU). FANCD2 provides a protection mechanism against genomic instability in cells lacking BRCA2 and its abrogation is lethal to these cells. Elevated apoptosis and reduced survival of BRCA2-compromised cells upon FANCD2 abrogation could be exploited therapeutically by treating BRCA2-deficient tumors with FANCD2 inhibitors.

Online methods

Cell lines and culture conditions

Human non-small cell lung carcinoma H1299 cells, human embryonic kidney HEK-293T cells, human mammary gland MDA-MB-231 cells, primary human fibroblast MRC-5 cells

(all from American Type Culture Collection) and colorectal adenocarcinoma DLD1 cells (parental and *BRCA2*-mutated, Horizon Discovery) were cultivated in monolayers in DMEM medium (Sigma Aldrich) supplemented with 10% fetal bovine serum (Life Technologies), 1% penicillin and streptomycin (Sigma Aldrich). H1299 and MDA-MB-231 cells expressing doxycycline (Dox)-inducible BRCA2 shRNA were established as previously described1. Cell lines were routinely tested for mycoplasma. H1299 and DLD1 cell lines were authenticated in February 2016.

Generation of *FANCD2*$^{-/-}$ cells by CRISPR/Cas9

FANCD2 double nickase plasmid (sc-400445-NIC) and FANCD2 homology-directed repair (HDR) plasmid (sc-400445-HDR) were purchased from Santa Cruz. DLD1 cells were transfected with 1 μg of each construct using Lipofectamine 2000 (Thermo Fisher Scientific). Media were replaced with antibiotic-free media 24 h after transfection. After 24 h, puromycin (2 μg/ml) was added for 72 h to select cells expressing Cas9 nickase. Cells were left to recover for six days before seeding for single cell cloning. Clones showing loss of all detectable FANCD2 by immunoblotting were selected for subsequent analysis.

RNAi

Cells were transfected with siRNA by reverse transfection using DharmaFECT 1 (Dharmacon). FANCD2 and BRCA2 siGENOME SMARTpool (used at 40 nM) were obtained from Dharmacon, FANCA and FANCD2 esiRNA (used at 20 nM) from Sigma Aldrich and AllStars negative control siRNA from Qiagen.

Clonogenic survival assays

Cells were plated in triplicate at densities between 200 and 1,000 cells per well in 6-well plates and drug treatment was initiated after cells had adhered. Following 24-h incubation with the drug, fresh media without the drug were added for 10-14 days. Colonies were stained with 0.5% crystal violet (Sigma Aldrich) in 50% methanol, 20% ethanol in dH_2O. Cell survival was expressed relative to untreated cells of the same cell line.

β-galactosidase assay

Cells were fixed with 2% formaldehyde, 0.2% glutaraldehyde for 10-15 min at room temperature and stained by incubation with freshly prepared staining solution (1 mg/ml X-Gal, 5 mM potassium ferrocyanide, 5 mM potassium ferricyanide, 150 mM NaCl, 2 mM MgCl2, 40 mM citric acid, pH 6.0) at 37ºC with atmospheric CO_2 levels. Staining was stopped after 6 h. Cells were examined using light microscopy. Number of cells analyzed per sample from three independent experiments: -Dox, -FANCD2 n = 2,342; -Dox, +FANCD2 n = 1,971; +Dox, -siFANCD2 n = 1,926; +Dox, +siFANCD2 n = 2,330.

Annexin V assay

Apoptotic and dead cells were labeled using the FITC Annexin V/Dead Cell Apoptosis Kit (Thermo Fisher Scientific) according to manufacturer's instructions. Stained cells were immediately analyzed by flow cytometry (FACSCalibur, BD Biosciences). Early apoptotic cells bound Annexin V-FITC but excluded propidium iodide (PI). Cells in necrotic or late

apoptotic stages were labeled with both Annexin V-FITC and PI. 20,000 events were analyzed per condition and experiment using FlowJo software.

Immunofluorescence

Cells were washed in PBS, swollen in hypotonic solution (85.5 mM NaCl and 5 mM $MgCl_2$) for 5 min, fixed with 4% paraformaldehyde for 10 min at room temperature and permeabilized by adding 0.03% SDS to the fixative. After blocking with blocking buffer (1% goat serum, 0.3% BSA, 0.005% Triton X-100 in PBS), cells were incubated with primary antibody diluted in blocking buffer overnight at room temperature. Then, they were washed again and incubated with fluorochrome-conjugated secondary antibody for 1 h at room temperature (1:300, anti-mouse Alexa 546, A-11003, Molecular Probes). Dried coverslips were mounted on microscope slides using ProLong Gold Antifade Mountant with DAPI (Thermo Fisher Scientific). Specimens were imaged using an LSM780 (Carl Zeiss Microscopy) confocal microscope and nuclei were analyzed using ImageJ software (NIH). Number of nuclei analyzed per sample from four independent experiments: -Dox, -siFANCD2 $n = 767$; -Dox, +siFANCD2 $n = 668$; +Dox, -siFANCD2 $n = 737$; +Dox, +siFANCD2 $n = 650$.

Preparation of metaphase spreads

Mitotic cells were collected by mitotic shake-off and swollen in hypotonic buffer (0.03 M sodium acetate) at 37ºC for 25 min, then fixed in a freshly prepared 3:1 mix of methanol:glacial acetic acid. Nuclear preparations were dropped onto slides pre-soaked in 45% acetic acid and stained with Giemsa. Metaphases were viewed with a Leica DMI6000B inverted microscope equipped with a HCX PL APO 100x/1.4-0.7 oil objective. Images were acquired using a Leica DFC350 FX R2 digital camera and LAS-AF software (Leica). Brightness levels and contrast adjustments were applied using Photoshop CS3 (Adobe). 60 metaphases from two independent experiments were quantified per condition.

DNA fiber assay

DNA was labeled with 25 μM CldU (5-Chloro-2′ -deoxyuridine) and 250 μM IdU (5-Iodo-2′-deoxyuridine) as outlined in the figures. HU was used at 2 mM and mirin at 50 μM. The reaction was terminated by addition of ice-cold PBS. After cell lysis, DNA was spread on glass slides, fixed in methanol/acetic acid, denatured with HCl, blocked with 2% BSA and stained with anti-rat anti-CldU (1:500, ab6326, Abcam, validated in Zimmer, et al. 1) and mouse anti-IdU (1:100, clone B44, 347580, Beckton Dickinson, validated in Zimmer, et al. 1) antibodies. Anti-rat Cy3 (1:300, 712-116-153, Jackson ImmunoResearch) and anti-mouse Alexa 488 (1:300, A-11001, Molecular Probes) were used as secondary antibodies. Images were acquired as described for metaphases and at least 200 tracks per condition from at least two independent experiments were analyzed using ImageJ software (NIH). Newly fired origins were defined as IdU track only. Exact numbers of tracks analyzed can be found in Supplementary Table 3-7.

Immunoblotting

Cells were harvested by trypsinization, washed with cold PBS, re-suspended in SDS-PAGE loading buffer, sonicated and boiled at 70°C for 10 min to prepare cell extracts. Equal amounts of protein (80-100 μg) were analyzed by gel electrophoresis followed by Western blotting. NuPAGE-Novex 3-8% Tris-Acetate gels (Life Technologies) were run according to manufacturer's instructions. Original, uncropped images of gels used in this study can be found in Supplementary Fig. 5.

Antibodies

The following antibodies were used for immunoblotting: rabbit polyclonal antisera raised against FANCD2 (NB100-182, Novus Biologicals, validated in Lossaint, et al. 7) and SMC1 (A300-055A, Bethyl Laboratories, validated in Zimmer, et al. 1), and a mouse monoclonal antibody raised against BRCA2 (OP95, Merck Millipore, validated in Zimmer, et al. 1). The secondary antibodies used were: polyclonal goat anti-rabbit immunoglobulins/HRP (P0448, Dako) and polyclonal goat anti-mouse immunoglobulins/HRP (P0447, Dako). A mouse monoclonal antibody raised against phosphorylated histone H2AX S139 (05-636, clone JBW301, Merck Millipore, validated in Zimmer, et al. 1) was used for immunofluorescence detection.

Genomic and transcriptional analysis in cell lines

Genomic data for a panel of 1,025 human cell lines was assembled from the COSMIC database16. Cell line pellets collected during exponential growth in RPMI or DMEM/F12 were used to generate microarray data using the Human Genome U219 array (Affymetrix). The robust multi-array analysis algorithm17 was used to establish intensity values for each of 18562 loci (BrainArray v.1018). The normalized data was then gene-wise normalized. Following this, the expression of each gene was centered across each tissue (0 mean and unitary standard deviation). Raw data was deposited in ArrayExpress (E-MTAB-3610). Driver mutations in *BRCA2* were defined as those that were truncating and therefore likely to result in a shortened translation product (frameshift, nonsense and essential splice mutations) or homozygous deletions at copy number level. These mutations where then correlated with *FANCD2* gene expression.

FANCD2 mRNA expression levels in tumors

Data of 971 human breast cancer/normal matched samples were considered from The Cancer Genome Atlas19. Expression of *FANCD2* mRNA was considered in samples with and without *BRCA2* somatic mutations. Equality of expression distribution was tested using a Kruskal-Wallis rank sum test (Kruskal-Wallis chi-squared = 10.043, df = 2, $p = 0.006596$).

Supplementary Material

Refer to Web version on PubMed Central for supplementary material.

Acknowledgements

We thank S. Bertrand for help with the senescence assays. We are grateful to G. Brown and M. Woodcock for their assistance with microscopy and FACS analyses, respectively. J.Z. is supported by a Cancer Research UK D.Phil.

Studentship. M.T. lab is funded by Cancer Research UK A17201, Medical Research Council, University of Oxford and the EMBO Young Investigator Programme.

References

1. Zimmer J, et al. Mol Cell. 2016; 61:449–60. [PubMed: 26748828]
2. Badie S, et al. Nat Struct Mol Biol. 2010; 17:1461–9. [PubMed: 21076401]
3. Schlacher K, et al. Cell. 2011; 145:529–42. [PubMed: 21565612]
4. Lomonosov M, Anand S, Sangrithi M, Davies R, Venkitaraman AR. Genes Dev. 2003; 17:3017–22. [PubMed: 14681210]
5. Schlacher K, Wu H, Jasin M. Cancer Cell. 2012; 22:106–16. [PubMed: 22789542]
6. Lachaud C, et al. Science. 2016; 351:846–9. [PubMed: 26797144]
7. Lossaint G, et al. Mol Cell. 2013; 51:678–90. [PubMed: 23993743]
8. Michl J, Zimmer J, Tarsounas M. EMBO J. 2016
9. Zeman MK, Cimprich KA. Nat Cell Biol. 2014; 16:2–9. [PubMed: 24366029]
10. Chaudhury I, Sareen A, Raghunandan M, Sobeck A. Nucleic Acids Res. 2013; 41:6444–59. [PubMed: 23658231]
11. Carlos AR, et al. Nat Commun. 2013; 4:2697. [PubMed: 24162189]
12. Chen YH, et al. Mol Cell. 2015; 58:323–38. [PubMed: 25843623]
13. Jackson SP, Bartek J. Nature. 2009; 461:1071–8. [PubMed: 19847258]
14. Nijman SM. FEBS Lett. 2011; 585:1–6. [PubMed: 21094158]
15. Kim Y, et al. Blood. 2013; 121:54–63. [PubMed: 23093618]
1. Zimmer J, et al. Mol Cell. 2016; 61:449–60. [PubMed: 26748828]
7. Lossaint G, et al. Mol Cell. 2013; 51:678–90. [PubMed: 23993743]
16. Forbes SA, et al. Nucleic Acids Res. 2015; 43:D805–11. [PubMed: 25355519]
17. Irizarry RA, et al. Biostatistics. 2003; 4:249–64. [PubMed: 12925520]
18. Dai M, et al. Nucleic Acids Res. 2005; 33:e175. [PubMed: 16284200]
19. Ciriello G, et al. Cell. 2015; 163:506–19. [PubMed: 26451490]

Europe PMC Funders Author Manuscripts

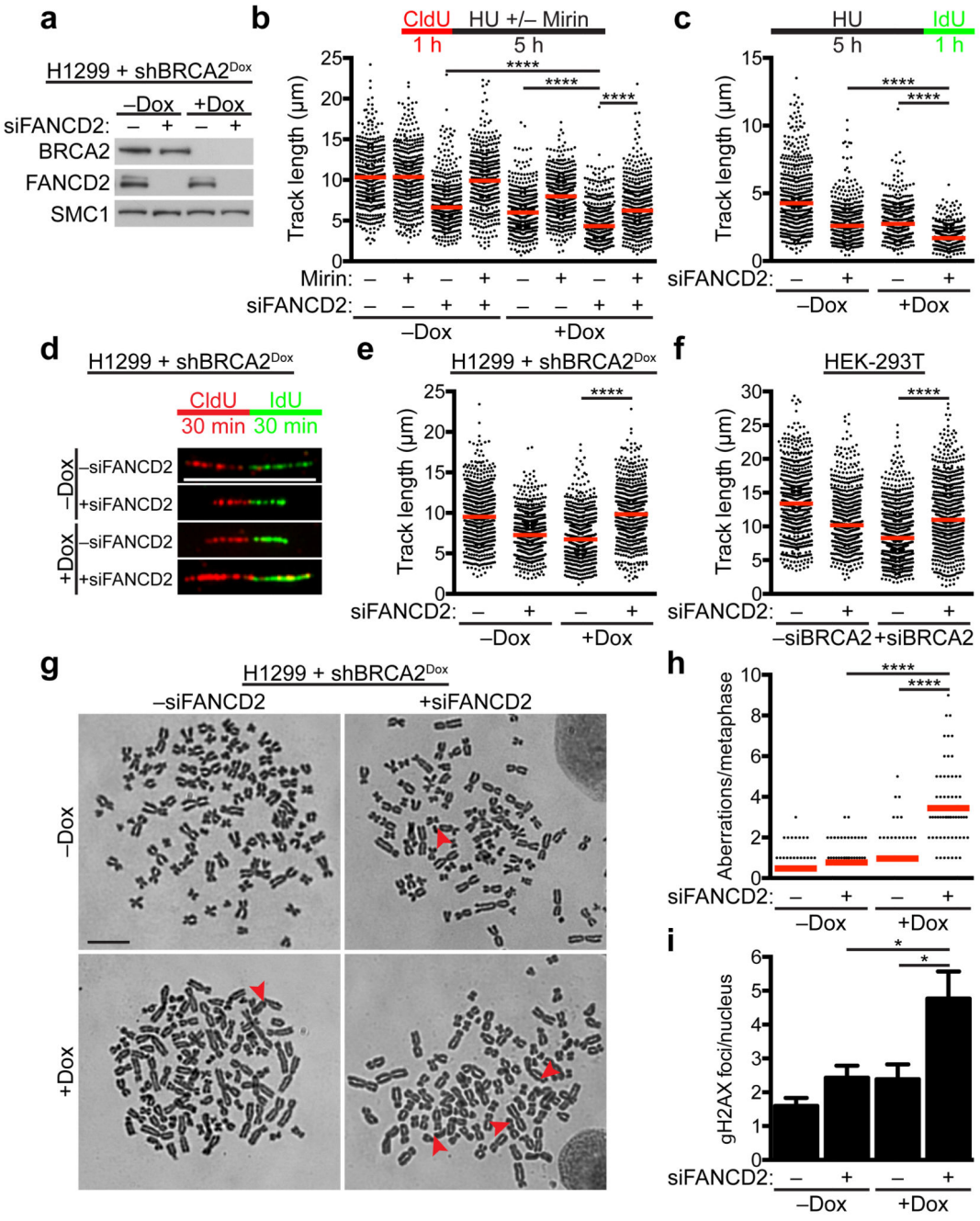

Figure 1.

FANCD2 restricts replication and prevents DNA damage accumulation in BRCA2-deficient cells. (**a**) Western blot showing FANCD2 siRNA-mediated depletion and BRCA2 knockdown by doxycycline (Dox)-inducible shRNA in H1299 cells. Uncropped blots are shown in Supplementary Fig. 5. (**b,c**) Quantification of fiber track length of H1299 cells treated as outlined in inset. Each dot represents one fiber. Number of fibers quantified from two independent experiments are listed in Supplementary Tables 3,4; ****, $p < 0.0001$ (Mann-Whitney test). (**d-f**) Representative images and quantification of fiber track length of

H1299 and HEK-293T cells treated as outlined in inset. Each dot represents one fiber. Number of fibers quantified from three independent experiments are listed in Supplementary Tables 5,6; ****, $p < 0.0001$ (Mann-Whitney test). scale bar, 10 μm. (**g**,**h**) Representative images and quantification of chromosomal aberrations per metaphase in H1299 cells. red bar, mean. Arrowheads point to aberrations. Each dot represents one metaphase. 60 metaphases from two independent experiments were quantified; ****, $p < 0.0001$ (Mann-Whitney test). scale bar, 10 μm. (**i**) Quantification of γH2AX foci per nucleus in H1299 cells. $n = 4$ (independent experiments); error bars, SEM; *, $p < 0.05$ (unpaired, two-tailed *t* test).

Europe PMC Funders Author Manuscripts

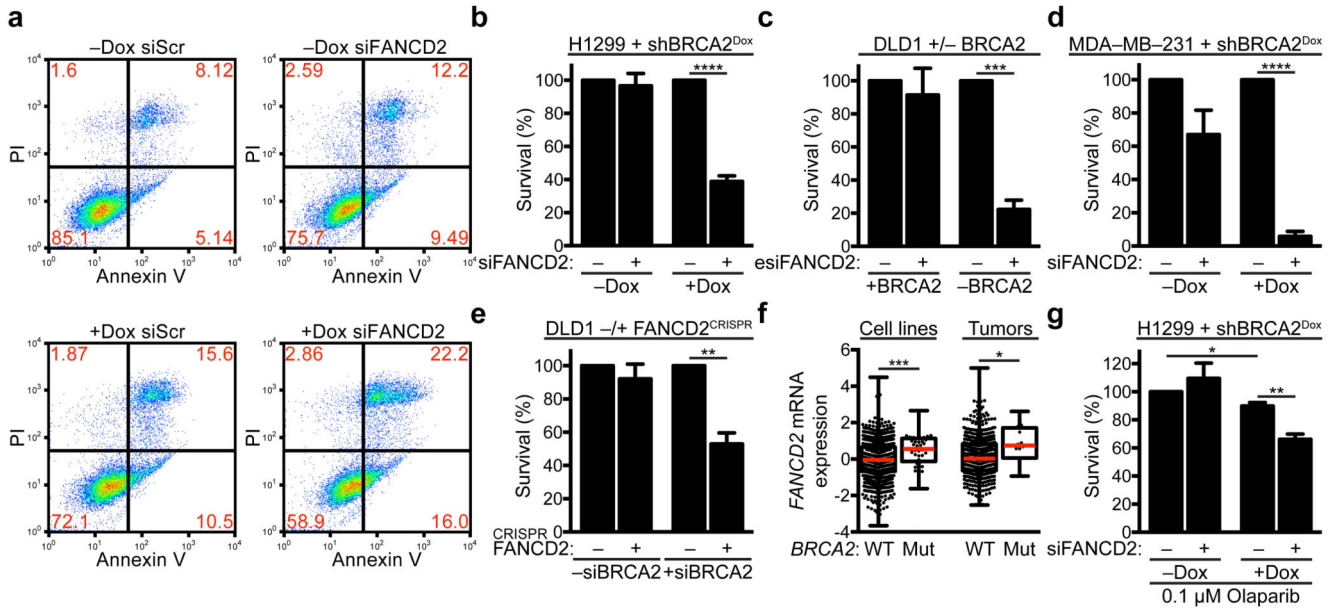

Figure 2.

FANCD2 is required for BRCA2-deficient cell survival and alters olaparib sensitivity. (**a**) Analysis of apoptosis by Annexin V staining in H1299 cells. Shown are representative graphs of four independent experiments. (**b-d**) Clonogenic survival assays in H1299, DLD1 and MDA-MB-231 cells lacking BRCA2. $n = 3$ (independent experiments); error bars, SEM; ***, $p < 0.001$; ****, $p < 0.0001$ (unpaired, two-tailed t test). (**e**) Clonogenic survival assays in FANCD2-deficient DLD1 cells. $n = 3$ (independent experiments); error bars, SEM; **, $p < 0.01$ (unpaired, two-tailed t test). (**f**) *FANCD2* mRNA expression in cell lines ($n = 976$ for WT, $n = 43$ for Mut) and tumors ($n = 497$ for WT, $n = 12$ for Mut). Dots in graphs represent individual cell lines and tumors. Middle line represents median, and the box extends from the 25th to 75th percentiles. The whiskers mark the minimum and maximum values. *, $p < 0.05$; ***; $p < 0.001$ (Mann-Whitney test). WT, wild type. Mut, mutated. (**g**) Clonogenic survival assay in olaparib-treated H1299 cells. $n = 3$ (independent experiments); error bars, SEM; *, $p < 0.05$; **, $p < 0.01$ (unpaired, two-tailed t test).

Europe PMC Funders Author Manuscripts